

Article

The Mechanism of Position-Mode Side Guide in Correcting Camber in Roughing Process of a Hot Strip Mill

Han-Kai Hsu and Jong-Ning Aoh *

Advanced Institute of Manufacturing with High-Tech Innovations AIMHI, Department of Mechanical Engineering, National Chung Cheng University, Minhsiung, Chiayi 62102, Taiwan; classmates319@gmail.com

* Correspondence: imejna@ccu.edu.tw; Tel.: +886-5-272-9218

Received: 23 February 2019; Accepted: 23 April 2019; Published: 29 April 2019



Abstract: The mechanism of the position-mode side guide in correcting slab centerline profile and camber in the roughing process of a hot strip mill (HSM) was analyzed using finite element simulation. The finite element model was established based on the actual size of the roughing mill and on the actual actuating time sequence of the roughing mill in China Steel Corporation (CSC), Kaohsiung. This work could be the first to give an insight into the mechanism of side guides in correcting the slab camber. Time sequence analysis was explored to visualize the progress of centerline profile variation and the interaction between the slab and the related roughing mill components at different moments. The history of reaction forces exerted on the slab was analyzed to explain the interaction between roughing mill components and the slab. The effect of the separation distance of side guide and the effect of the slab wedge on the centerline profile was investigated. A schematic model illustrating the reactions and the resulting moments exerted on the slab was created. By examining the force history, the cross-sectional strain/stress distribution, and the roll force across the horizontal roller, the correcting mechanism of the side guide could be elucidated. The simulation results provide further knowledge in selection and dimension design of side guide to improve the effectiveness of side guide in correcting the slab profile.

Keywords: position-mode side guide; hot strip mill; roughing process; slab wedge; slab camber; finite element modeling

1. Introduction

High-strength steel sheets with reduced gauge thickness have become a significant trend in sheet steel products due to increasing lightweight applications in the automobile, vehicle and structure industry. Therefore, a precise and stable hot rolling process is highly demanded. The slab or strip profile control and the process stability are crucial to the quality of the product and the production flexibility of the hot strip mill. The dimension and profile of the slab, the arrangement of the rollers, the edger and auxiliary components such as side guides, and the program control logic of roughing and finishing mills have significant influence on the quality of the semi-product or end product of hot rolling process. In fact, the quality of hot strip mill products is directly reflected by the final profile and geometry of the slab or strip which also has a decisive influence on the production efficiency and yield rate. Asymmetric profiles such as camber and wedge are usually an accumulative outcome resulting from consecutive continuous or reverse rolling passes. During hot rolling, steel slabs are milled under large reduction from a large thickness down to relatively small gauges. Inappropriate process conditions such as temperature differences over the slab width, horizontal roller misalignment, and lateral shift of the slab would lead to camber and deviation of the centerline profile. These asymmetric strip

geometries would seriously influence the process stability and the product quality of the subsequent finish milling.

A hot rolling production line generally consists of several main stands beginning from the heating furnace, roughing mill, finishing mill, laminar cooling to down coil, as shown in Figure 1. The heating furnace is usually located at the drive side (DS) of the production line. The drive side is defined as the side where the driving motors of horizontal rollers are installed. The other side of the production line is called the work side (WS) where the change of rollers and maintenance of mill stands takes place. The slab may experience temperature differences over the width of the slab after moving out from the furnace to the conveyer prior to roughing process, as schematically revealed in Figure 2. The temperature differences result in a gradient and differences of elastic and plastic flow properties over the width of the slab. A roughing line primary consists of several pairs of horizontal rollers (roughing rolls) to reduce the thickness and vertical rollers (edging rolls) to control the width of the slab. The aforementioned gradient in properties may cause asymmetric material flow over the width of the slab and subsequently lead to camber of the slab [1,2], as depicted in Figure 3. The phenomenon may even become severe during the multi-pass roughing process. Camber of a slab can be defined quantitatively as the largest off-centering between the curved centerline and the initial straight centerline of a slab. Initial wedge of a slab over the width also causes camber after the roughing process.

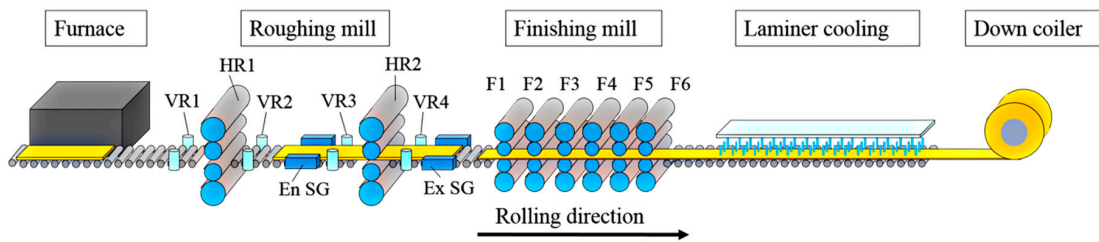


Figure 1. Schematic layout of hot rolling production line.

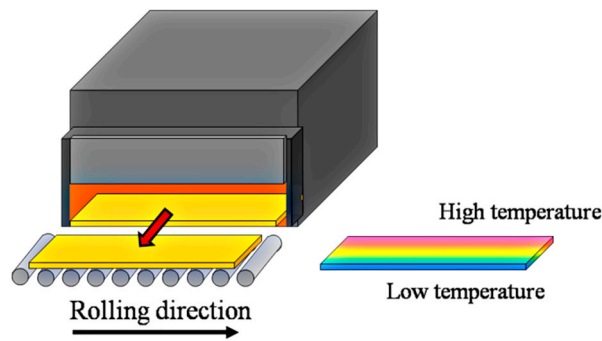


Figure 2. Schematic illustration showing temperature gradient of a slab over the width while the slab moving out from furnace to the conveyer.

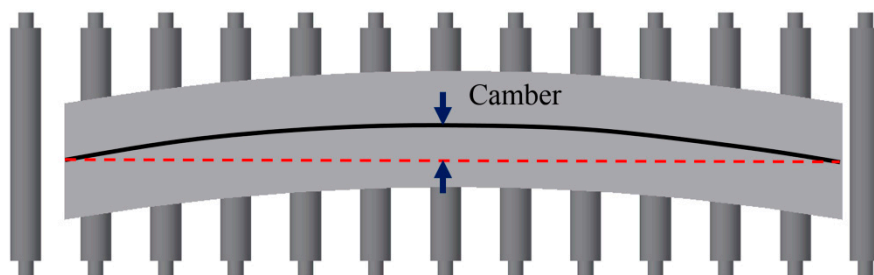


Figure 3. Schematic top view of the cambered slab.

Generally, the curvature of the slab centerline can be controlled by adjusting the tilt angle between the horizontal roller pair of the roughing stands so that the difference in material flow rate over the slab width can be reversely compensated by the slight difference in reduction over the horizontal roller gap [3,4]. The slab form can be modified or corrected by the technique of continuous variable crown (CVC) of the work rolls [5,6]. In finishing mill stands, however, tilt angle control and differential force control are quite sophisticated and require very fast response due to the elevated rolling speed of the thinning strip and multiple close-to-one-another mill stands [7–11].

A pair of entrance side guides (En SG) before the vertical edging rolls (VR3) and a pair of exit side guides (Ex SG) after the vertical edging rolls (VR4) of the roughing stand 2 (HR2) are installed, as shown in Figure 1. These side guide pairs bear the basic function of ensuring smooth entering and outgoing of the slab, maintaining the slab motion along the centerline of the roughing mill by narrowing or widening the separation distance of the side guide arms. In addition, these side guides are effective in position adjustment to prevent the incoming or outgoing slab from lateral shift in the roughing mill stand. Furthermore, they are effective, when necessary, in correcting the centerline profile to reduce the camber by exerting a lateral force on the slab [12]. The side guide control is usually combined with horizontal roll alignment control and can be carried out in position-mode or in force-mode by hydraulic devices connecting to the side guide pair.

Although the entrance and exit side guides had been widely applied between roughing stands, there have been very few papers or literature examining the mechanism of side guides in correcting the slab curvature. Among the very few available papers, only the work of Byon et al. [13] focused on the design of guiding rollers, which were arranged on the inner flank of the side guides. Looking at the layout of the roughing mill in Figure 1, it is straightforward to think that the mechanism of correcting the slab curvature could not be realized by the side guides alone. The horizontal rolls and the edging rolls also simultaneously play a certain role in the correction mechanism. Therefore, this work was focused on the analysis of the mechanism of the side guides and the associated roughing mill components, which participate in correcting the camber of the slab during the roughing process. Only position-mode side guide was taken into account in this research.

2. Working Principle of Side Guide

The side guide is used to ensure smooth entering and outgoing of the slab, to maintain the slab motion along the centerline of the roughing mill. Entrance and exit side guides are located before and behind roughing rolls as depicted in Figure 1. Prior to the head of the slab entering the entrance side guide or exit side guide, the initial separation distance of the side guide must be wide enough to avoid undesirable contact of the slab head against the inner flank of the side guide during entering. Some side guide devices are designed to have a conical opening at the run-in side. As the slab is further conveyed into the region confined by the side guide, the separation distance of side guide is reduced to an amount of slab width plus a reasonable gap between the slab and the inner flanks of the side guide. If the slab becomes cambered during the roughing pass, the outgoing slab may bend to one side and contact the inner flank of the exit side guide. The lateral contact pressure of the exit side guide exerting on the slab as force, and the horizontal roll-bites and the vertical edging rolls as pivot, results in a moment and tends to rotate or to deflect the outgoing slab. Therefore, the centerline profile or camber is corrected until the slab is completely disengaged from the exit side guide. The schematic illustration of the sequence of side guide motion is shown in Figure 4.

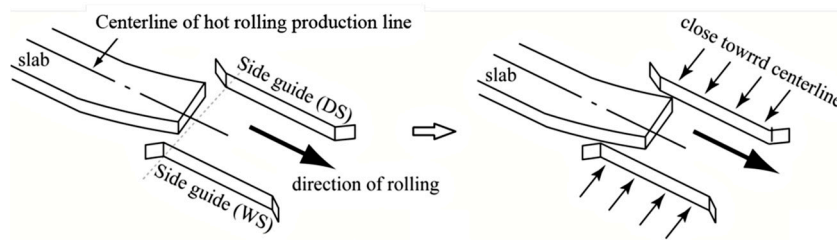


Figure 4. Schematic illustration of the sequence of side guide motion.

3. Finite Element Modeling and Methodology

3.1. Slab Modeling

The finite element model consists of roughing rolls, edging rolls, and the entrance and exit side guides. The dimensions were based on the actual size layout of the No. 2 roughing mill (R2) in China Steel Corporation (CSC), Kaohsiung. To satisfy the slab geometry when passing through the second roughing mill stand, the slab model was set to 10 m long, 1.2 m wide, and 22 cm thick as shown in Figure 5. To ensure that contact between the side guide and the slab must occur in the simulation, the length of the slab should be at least 8 m. The purpose of this work was to investigate the effect of the side guide in correcting the camber of the slab in trend. In order to be able to reduce the simulation time, and nevertheless to obtain reasonable computation results to show the detail of camber, an initial slab length of 10 m was chosen. The slab model was given different initial wedges of 1 mm, 0.8 mm and 0.5 mm with the work side (WS) slightly thicker than the drive side (DS). Different degrees of wedge would result in different shapes of camber after the slab passes the roughing rolls. In order not to mix the effect of initial wedge and the effect of initial camber in the R2 roughing mill, we neglected the slab camber after first roughing mill (R1) and assumed a camber-free slab prior to roughing in R2.

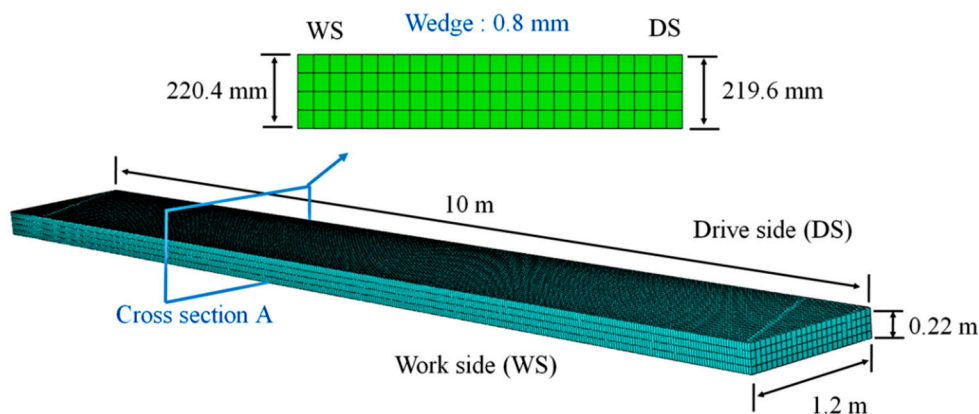


Figure 5. Finite element modeling of slab.

The slab model was divided into 1000, 24 and 4 elements along the longitudinal, width, and thickness direction, respectively. There were 38400 elements in total. The 3D element type C3D8RT was chosen. The dimension of elements was 25 mm (L) \times 50 mm (W) \times 55 mm (t). Uniform temperature distribution prior to rolling was assumed. The initial temperature of the slab was chosen at 1100 °C.

3.2. Roughing Mill and Side Guide Modeling

As depicted in Figure 1, a four-high mill consists of a pair of back-up rolls and a pair of work rolls. Although the amount of elastic deformation of the work rolls is in general very small, it may not be neglected in some cases such as the cold rolling of strips using CVC rolls [14,15] since it would affect the thickness uniformity of the strip under cold rolling. In addition, in the case of the simulation of a

deep drawing process [16], although the elastic deformation of the press/die was small, it could not be neglected since it was still in the order of the magnitude of the deep-drawn part tolerance. In the case of the roughing process, the function of the back-up rolls is to suppress the work roll from large elastic bending during rolling. Being extremely small compared with the global plastic deformation of the slab, the elastic deformation of the work rolls can be neglected in the modeling, and consequently, the work rolls were considered as rigid. Therefore, the No. 2 roughing mill model can be simplified as consisting of a pair of work rolls (HR2), two pairs of vertical rolls (VR3 and VR4) and two pairs of side guides, as shown in Figure 6. All these components were regarded as rigid. In order to investigate the rolling force distribution over the work rolls, nine rigid shell elements over the width were given to the work roll model. The dimensions of the components are listed in Table 1. The rolling parameters were adopted from the No. 2 roughing mill in CSC and are summarized in Table 2.

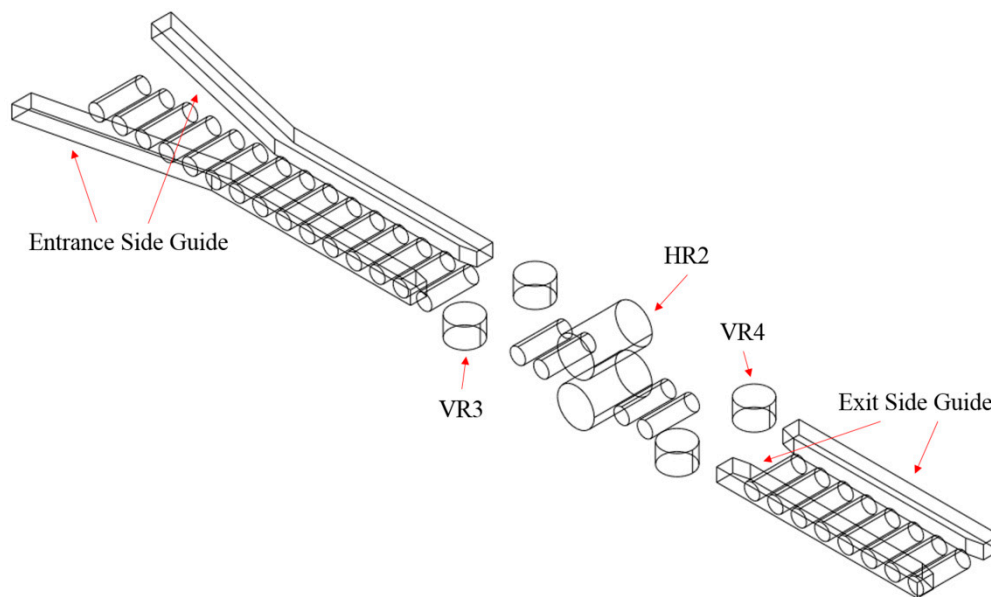


Figure 6. Schematic modeling of roughing rolls, edging rolls, and side guides.

Table 1. Dimensions of the roughing mill components and side guide.

Model	Dimensions
Work rolls (HR2)	Length: 2 m/Diameter: 1.1 m
Vertical rolls (VR3/VR4)	Diameter: 0.92 m
Entrance side guide (En SG) separation	1210/1214 mm
Exit side guide (Ex SG) separation	1220/1224 mm

Table 2. Roughing parameters.

Roughing Parameters	Value
Traverse speed	2.3 m/s
Work rolls (HR2) reduction	0.18
Vertical rolls (VR3) reduction	0.016
Work rolls (HR2) friction coefficient	0.45
Vertical rolls (VR3) friction coefficient	0.3

The entrance side guide (En SG) is located before VR3 and the exit side guide (Ex SG) is located behind VR4. With the support of the hydraulic system, the side guide deformation and displacement caused by the contact between the side guide and the slab are very small in the roughing practice and thus can be neglected. Therefore, the side guide model was also regarded as rigid. As the slab is conveyed into the side guide, the separation distance of side guide is reduced to an amount slightly

larger than the slab width. In this work, as the slab width is 1200 mm, the entrance separation distance of side guide was set at 1210 mm and 1214 mm. As the initial slab is camber-free, the slab was able to pass the entrance side guide without contacting the inner flank of the side guide. Since the slab experienced a lateral spread of 10 mm after roughing, the separation distance of the exit side guide should be larger than that of the entrance side guide. It was set at 1220 mm and 1224 mm. In other words, the gap between inner flank of the side guide and one side of a slab was set at 5 mm and 7 mm, respectively. Figure 7 shows the coordinate positions of the roughing/edging rolls and side guides. The roughing rolls HR2 are located at the origin of the coordinates, two pairs of edging rolls are located at $x = \pm 3.135$ m. The entrance side guide is 10 m long and is located at $x = -14.58$ to $x = -4.58$ m. The exit side guide is 6 m long and is located at $x = 4.57$ to $x = 10.57$ m.

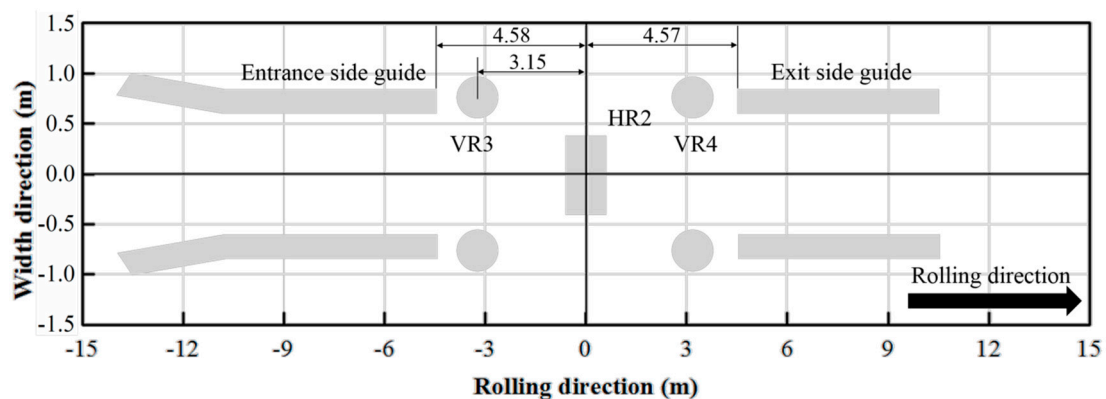


Figure 7. Top view showing coordinates of roughing rolls, edging rolls, entrance side guide, and exit side guide.

3.3. Actuation Sequence of Side Guides

Figure 8 illustrates the actuation sequence of side guides and the corresponding time sequence during the roughing process. Upon the slab entering the side guide, the separation distance of the entrance side guide reduced from 1300 mm to 1210/1214 mm at $t = 0-0.5$ s. The slab head entered VR3 at $t = 0.4$ s as labeled ① and then entered the roughing rolls HR2 at 1.9 s as labeled ②. Upon the slab head further entering the exit side guide at $t = 4-4.5$ s, the separation of the exit side guide reduced from 1300 mm to 1220/1224 mm. The side guide arms remained in contact with the slab. At $t = 5.3$ s, the slab end was disengaged from VR3 as labeled ③ and eventually left HR2 at 6.8 s as labeled ④.

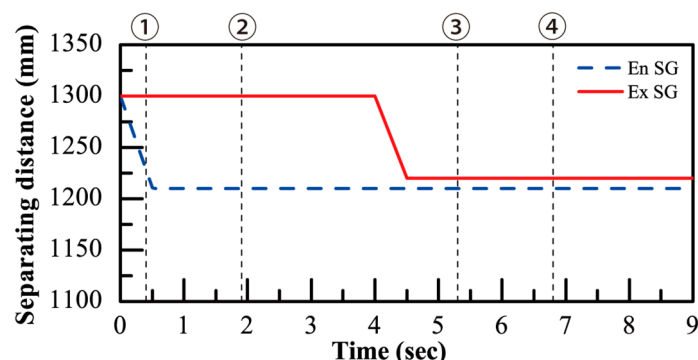


Figure 8. The actuation sequence of the side guide and the corresponding time sequence of slab motion.

3.4. Material Flow Curves of SAE1016

Considering the roughing process parameters and on-site data available from the production line of CSC, SAE1016 low carbon steel was chosen for the study. The flow curves were obtained

from a dynamic upset compression test using a GLEEBLE 3500 simulator under various strain rates. The specimens for the compression test were sampled from the strip semi-product after the roughing process. This was to ensure that the flow curves used in the computation were identical to those of the actual strips that experienced the real roughing process. The specimens had an initial length of 12 mm and diameter of 8 mm. The compression was conducted to an ultimate state with a final length of about 5 mm. The working temperature of the roughing process usually lies between 1100 °C and 950 °C, in addition, the working temperature of the strip at No. 2 roughing mill was approximately 1080 °C. Therefore, 900 °C and 1100 °C were chosen as the temperatures for the compression test to comply with reality.

The specimens were heated to the test temperatures, and held for about 1 min to ensure the uniformity of temperature. The strain rates of 0.1, 1, 20, 50 and 100 s⁻¹ were chosen for the compression test. The resulting flow curves are shown in Figure 9 and were applied as the constitutive model in the finite element computation. Interpolation or extrapolation of the flow curves was applied for temperature and strain rate conditions in-between. The SAE1016 steel has a density of 7832 kg/m³ and a Young's modulus of 213 GPa and 97 GPa at room temperature and at 900–1100 °C, respectively. The Poisson ratio is 0.33.

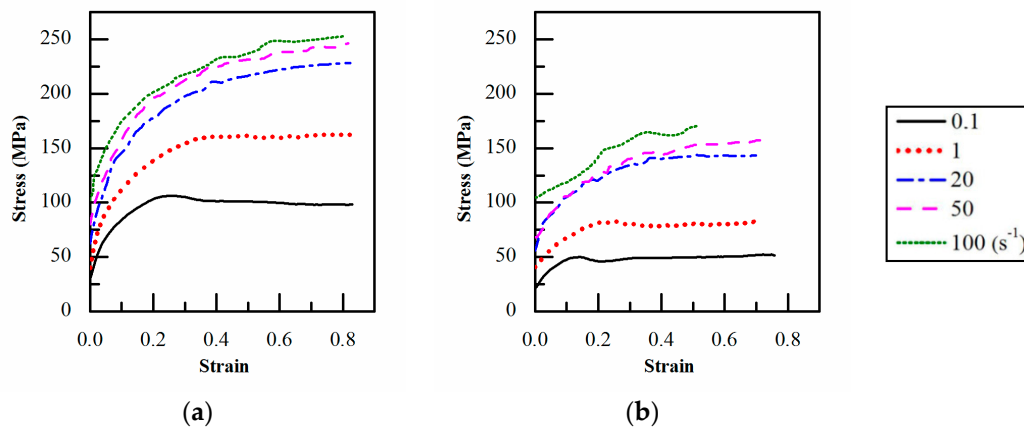


Figure 9. Flow curve of SAE1016 low carbon steel obtained from a GLEEBLE compression test; (a) 900 °C; (b) 1100 °C.

The explicit solver of ABAQUS was used to solve the dynamic deformation problem. Time sequence analysis showing consecutive sequence during the roughing process was explored. The slab centerline profile at different time sequences and the effect of the separation distance of the side guide on the slab centerline profile was predicted. The reaction history at the contact between the side guide and the slab, the force distribution across the horizontal rolls, and the strain and stress distribution across the transverse section of the slab at roll-bite were analyzed. With the results of the FE-analysis, the mechanism of the side guide and the associated devices in correcting the slab centerline curvature was proposed and elucidated.

4. Results and Discussion

4.1. Time Sequence Analysis of the Slab under Roughing Process

Time sequence analysis was explored to unveil the instantaneous contact between the slab and the side guide and rollers on one hand, and to reveal the resulting slab deformation by showing the centerline profile of the slab, on the other hand. Figure 10 shows the 3D-views of the slab at four consecutive time sequences at 2.5 s, 4.3 s, 4.7 s, and 6.2 s during roughing process. The slab entered into roughing rolls HR2, as shown in Figure 10a. Then the slab ran half-length through roughing rolls HR2 and entered into exit side guide while the slab end remained engaged in the entrance side guide,

as shown in Figure 10b. Figure 10c shows the moment immediately before the slab end leaves the edging rolls VR3 at 4.7 s. At this moment, the roughing rolls HR2 acted as pivot and one of the edging rolls VR3 exerted a reaction against the slab end. Eventually, the slab end completely disengaged from VR3 and was about to leave the roll-bite HR2 in Figure 10d.

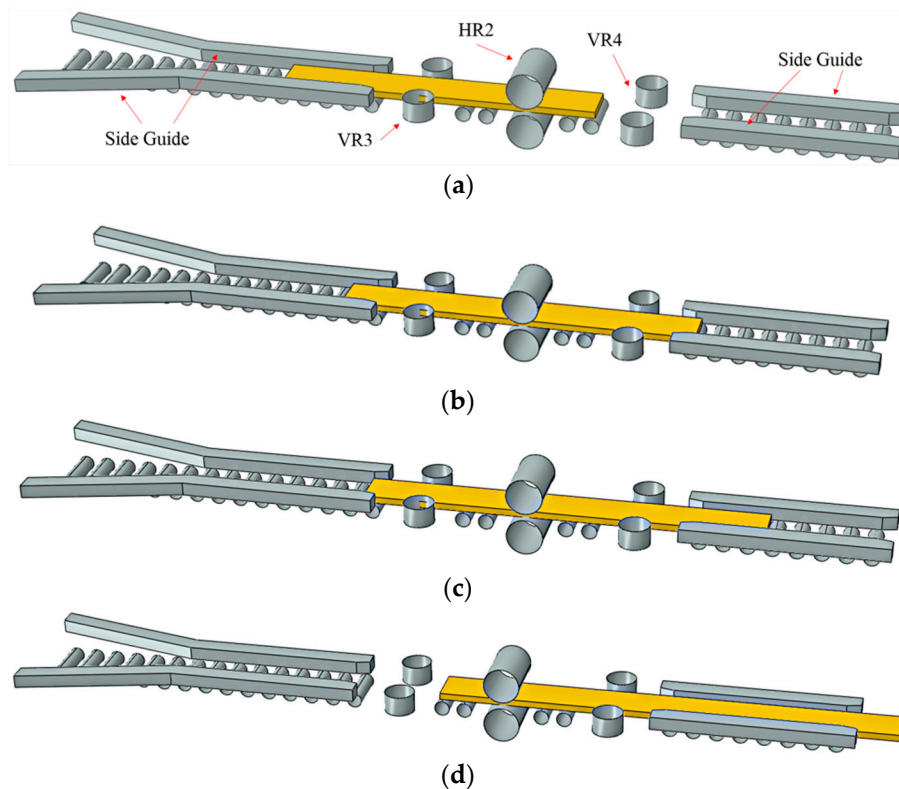


Figure 10. 3D schematic view of the finite element model showing slab position at different moments. (a) 2.5 s, the slab just entered the roll-bite. (b) 4.3 s, the slab head entered and touched the exit side guide. (c) 4.7 s, shortly before the slab end left the vertical edging rolls (VR3). (d) 6.2 s, the slab end is disengaged from VR3.

Figure 11 shows the instantaneous clips of the slab centerline profile at different moments. Relative to the size of the slab, the amount of camber and the size of the gap between the side guide and the slab are too small to be visually perceptible. We intentionally magnified the scale of the camber (centerline deviation) along the width direction in Figure 11 so that the camber and the centerline deformation are visually perceptible in the figure. At 2.5 s, the slab head was slightly cambered to the DS after passing through the roll-bite HR2 due to the initial wedge at the WS, as shown in Figure 11a. With the process of roughing, the centerline became cambered after the slab left the roll-bite. Eventually, the slab head was in contact with the side guide at about 4.3 s as revealed in Figure 11b. Immediately upon touching, the position-mode side guide arms began to close from the initial separation of 1300 mm to 1220/1224 mm. A side guide arm pressed at the slab head and restrained the slab from free cambering. At 4.7 s, as the side guide closed further, the slab centerline was deflected to the opposite side and became a deflected profile as depicted in Figure 11c. At this moment, the edging rolls VR3 exerted a reaction against the slab end. Eventually, the slab end completely left the entrance side guide and VR3 at 6.2 s and was about to leave the roll-bite. The centerline exhibited a deflected profile shown in Figure 11d. Note that the slab did not contact VR4 since VR4 is only actuated during reverse roughing and remains opened upon forward roughing.

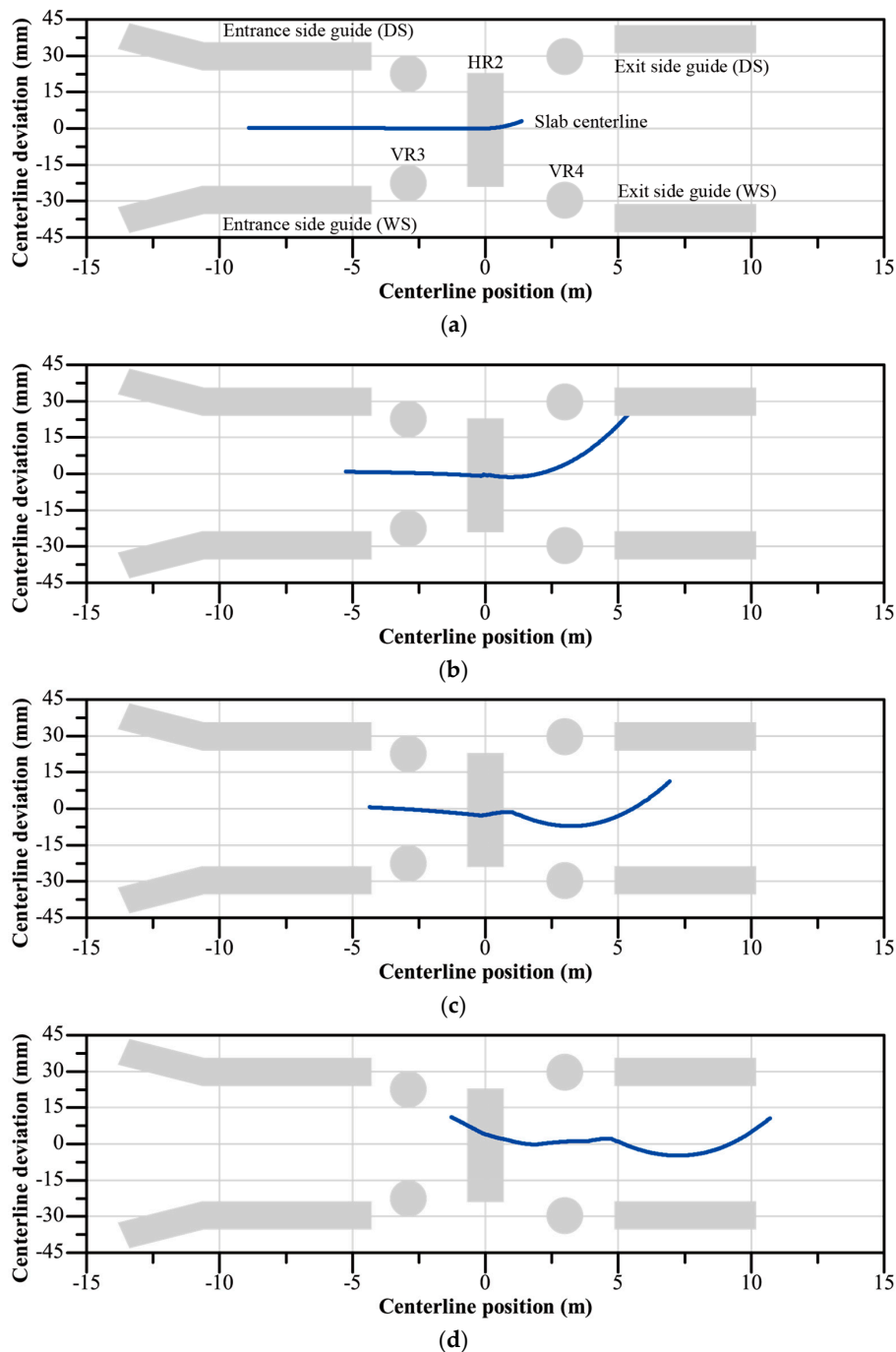


Figure 11. Instantaneous clips of the slab centerline at (a) 2.5 s, the slab did not touch the exit side guide; (b) 4.3 s, the slab head touched the exit side guide; (c) 4.7 s, shortly before the slab end disengaged from VR3; (d) 6.2 s, the slab end left VR3 and was about to leave roll-bite.

Corresponding to Figures 10 and 11, the force history exerted on the slab by the exit side is illustrated in Figure 12. As the slab head touched the DS of exit side guide at 4.3 s, a force peak of about 90 t was exerted on the slab (black dotted line). Then the side guide arm forced the slab to bend toward the WS, then the slab touched the WS of side guide at about 4.6 s and had a reaction of about 100 t exerted on the slab (red dotted line). Both DS and WS side guide arms continued to force the slab moving along the roughing centerline, the side guide arms on both sides exerted continuous contact force on the slab during 4.7 s and 6.6 s.

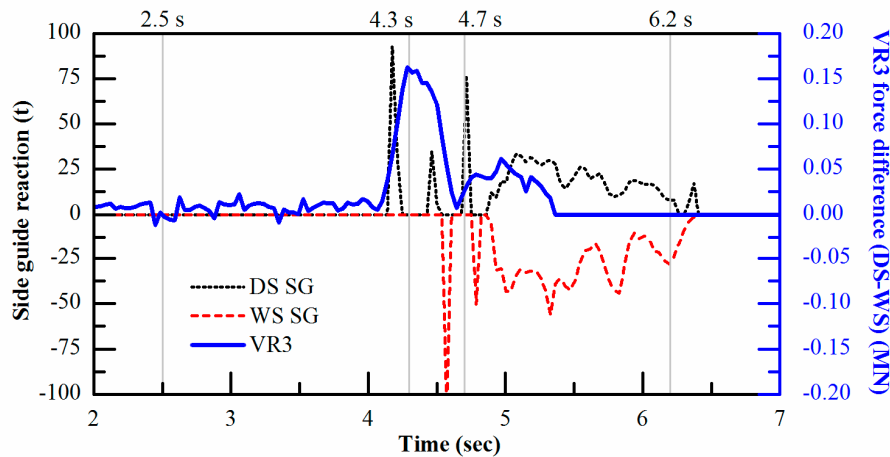


Figure 12. The reaction history of the exit side guide and VR3 vertical rolls.

It is worthwhile to note that during the period between 4.3 s and 5.3 s the slab head was continually pressed by the DS side guide arm, the slab tended to rotate due to a resultant moment about the contact (pivot) at roll-bite HR2. At the same time, the slab being vertically edged between VR3 rolls, tended to rotate toward the vertical roll at the DS. This would cause a greater reaction on the drive side vertical roll than on the work side vertical roll as schematically illustrated in Figure 13. The greater reaction on the DS vertical roll can only be made noticeable when we investigate the force difference between the DS and WS vertical rolls of VR3. In Figure 12, the force difference is expressed as a blue solid line. It shows a greater force difference of a maximum of 0.15 MN in magnitude on the DS. Upon the slab end completely leaving the VR3 at 5.3 s, the force difference immediately reduced to zero. The reaction history of the exit side guide and VR3 vertical roll in Figure 12 was a good interpretation of the interactions that had taken place between the slab and the roughing mill components illustrated in Figure 11. The results together with the schematic illustration in Figure 13 also elucidated the mechanism of the change or correction of the centerline profile at various moments.

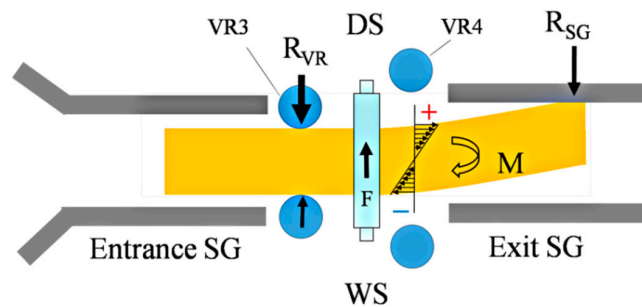


Figure 13. Schematic presentation of reactions and moment exerted on the slab due to interaction with the side guide and vertical roll.

4.2. The Effect of Side Guide in Correcting the Centerline Profile

It was found in Section 4.1 that the centerline profile of the slab had changed due to successive interaction between the slab and the roughing mill components. Now we further examine the effect of the separation distance of the side guide on the profile change and on the amount of camber of the slab. The amount of camber is defined here as the maximum deviation of the cambered centerline profile from the straight line connecting the slab head center point and the slab end center point. Figure 14 depicts the effect of the separation distance of the side guide on the amount of camber and on the centerline profile after roughing. The head and end of centerlines were made in coincidence with the centerline of the roughing mill so that the possible side walk of the slab was not taken into account.

The length is expressed in a dimensionless unit. With the preset wedge of 1 mm, the slab experienced a camber of 48 mm after roughing at 18% reduction if there is no exit side guide installed behind the roughing mill stand and an unrestrained development of centerline profile is allowed. In contrast, with the exit side guide installed, the amount of camber was effectively reduced from 48 mm to 20.7 mm and 16.3 mm if the slab was corrected by the exit side guide, with a separation distance of 1224 mm and 1220 mm, respectively. As depicted in Figure 14, the centerline profiles exhibited a slight “wavy” shape. It is reasonable to expect that the narrower the separation distance of side guide, the more effectively the side guide could correct the amount of camber and improve the centerline profile. The deflection of centerlines has been interpreted by considering the reactions exerted on the slab.

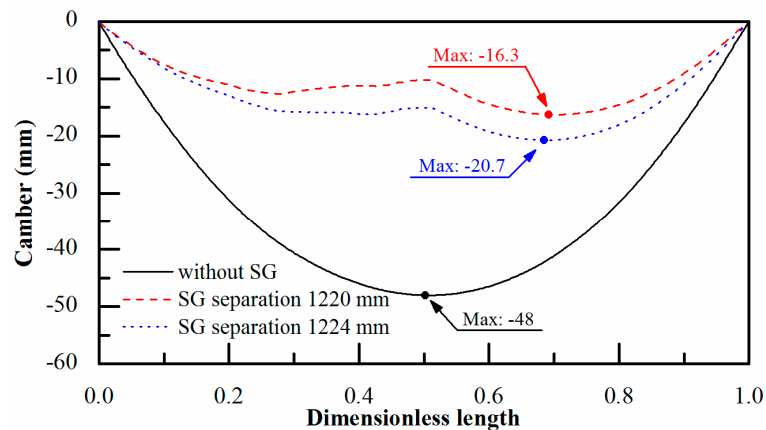


Figure 14. The effect of the separation distance of the side guide on the amount of camber and on the centerline profile after roughing (initial wedge: 1 mm, initial side guide opening: 1300 mm).

The effect of the amount of wedge of the slab on the camber and on the centerline profile is illustrated in Figure 15. The separation distance of exit side guide was set at 1220 mm. The amount of wedge was set at 1 mm, 0.8 mm and 0.5 mm. After roughing, the resulting maximum camber was 16.3 mm, 16.4 mm and 9 mm, respectively. The amount of camber and the centerline profile are almost identical for wedge of 0.8 mm and 1.0 mm. In general, the smaller the wedge, the smaller the camber would be. Although controlling the separation distance of position-mode side guide is a straightforward measure, the simulation results showed that adjusting the separation distance of side guide is a simple yet effective measure in reducing the camber and correcting the centerline profile of a slab.

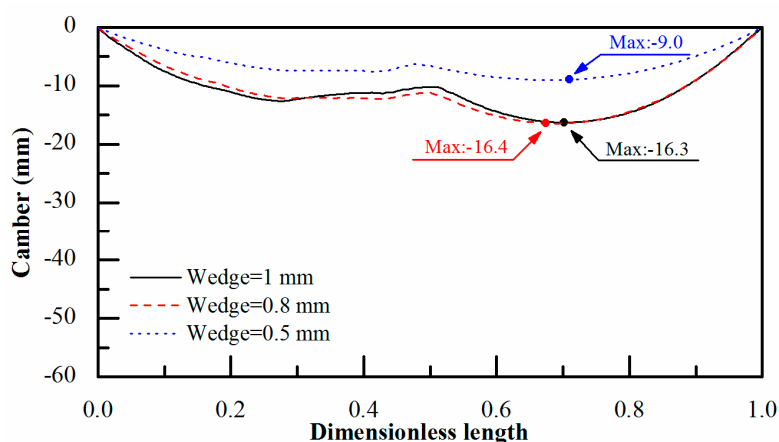


Figure 15. The effect of the slab wedge on the amount of camber and on the centerline profile after roughing. Initial separation distance of exit side guide: 1300 mm, final separation distance of exit side guide: 1220 mm.

A centerline profile of a slab plotted from on-site data of the No. 1 hot rolling line in CSC, Kaohsiung expressed as dimensionless length is compared with a simulated centerline profile in Figure 16. In both cases, the gap between the side guide arm and slab was kept at 5 mm. Note that the length of the slab was expressed as dimensionless length since the simulated slab and the actual one were not of the same length. They were 12 m and 20 m after R2 rolling, respectively. Therefore, they were consistent with each other in the trend of camber and in the characteristic of deflection in the middle region of the slab instead of in the actual value of length or amount of camber. The amounts of camber in the middle region of both curves were of the same order of magnitude. In fact, the amounts of camber were less than 30 mm in both cases. The values were relative small in comparison with the slab length of more than 12 m.

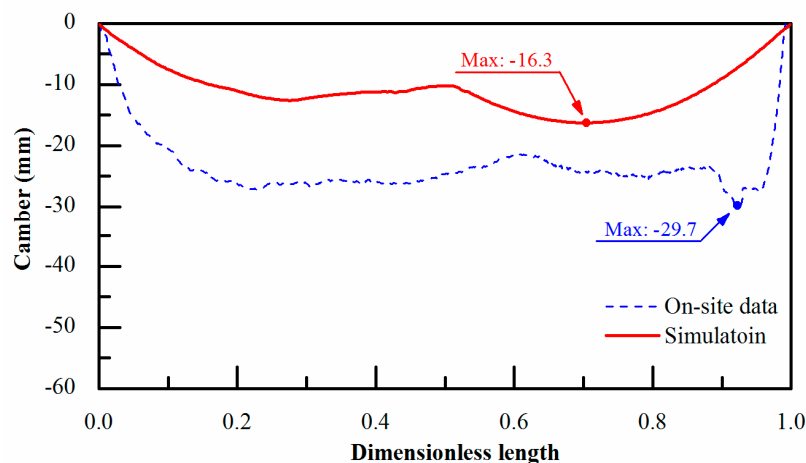


Figure 16. Comparison of a centerline profile plotted from on-site data with a simulated centerline profile. Separation distance of side guides: 1220 mm in both cases.

The centerline of the slab from on-site data however, shows profound head and tail camber due to the initial profile of the actual slab. The maximum head camber was about 29.7 mm. As soon as the slab head is disengaged from the exit side guide, or the slab end is disengaged from the vertical rolls VR3, the resultant moment becomes zero. The side guide is indeed less effective in correcting the head and tail camber in the roughing mill practice. In addition, multi-pass roughing of the actual slab also could be a reason for the difference between these two profiles. With this comparison, the numerical side guide model in predicting the camber profile and in simulating the correction of centerline profile during the roughing process is verified.

4.3. Strain and Stress Distribution on the Slab and Force Distribution on the Roughing Rolls

As illustrated in Figure 13, the slab tended to be rotated by a resultant clockwise moment about the pivot at roll-bite HR2. At the same time, being vertically edged between VR3 rolls, the slab end tended to rotate CW toward the drive side vertical roll VR3. The stress distribution at the exit cross-section of the slab directly under the roll-bite due to the applied moment is schematically illustrated in Figure 13, with longitudinal tensile stress distributed on the DS and compressive stress on the WS.

Now we consider the strain and stress distribution at the exit cross-section of the slab under rolling pressure as well as under the resultant moment. Figure 17 shows the strain and stress distribution without the constraint of the side guide. An initial wedge of 1 mm on the WS would cause a gradient of material flow under the roll-bite and leads to a deflection of the slab head toward DS as mentioned in Section 4.2. Figure 17a–d shows larger longitudinal stretch strain (ϵ_{11}) at WS than at DS due to the material flow gradient at different moments. Figure 17e–h shows generally a symmetric compressive rolling stress distribution over the width of slab during rolling as the slab was not constrained by the side guide.

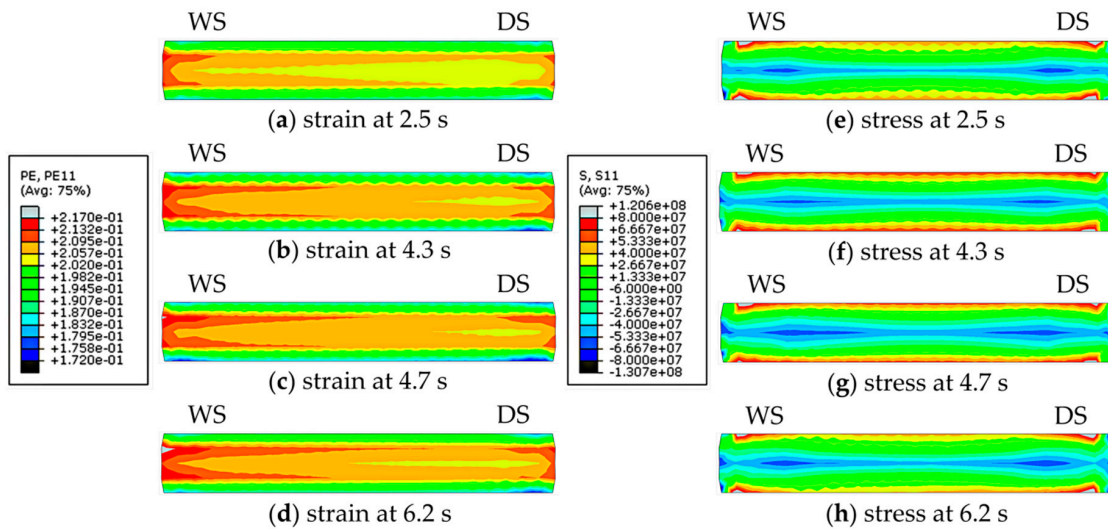


Figure 17. Strain and stress distribution at the exit cross-section of the slab being rolled without the side guide.

With the side guide installed, Figure 18 shows the strain and stress distribution under the combined loading of rolling pressure and the moment exerted by the exit side guide. Corresponding to the time sequence analysis of centerline camber shown in Figure 11, the slab head first freely cambered toward the DS in the initial stage of rolling, thus a larger longitudinal stretch strain (ϵ_{11}) resulted at the WS up to 2.5 s, as shown in Figure 18a. Then beginning from 4.3 s, with the reaction of the exit side guide exerted on the slab head, the slab head was deflected toward the WS, larger longitudinal stretch strain was at the DS than at the WS from 4.3 s to 4.7 s, as revealed in Figure 18b,c. Figure 18d shows that the WS exhibited slightly larger longitudinal stretch strain again at 6.2 s when the slab was constrained by both the WS and DS side guide arms. The corresponding stress distribution is illustrated in Figure 18e–h. It is worthwhile to note that during the period between 4.3 s and 4.7 s, larger combined compressive stress appeared at the WS due to the correcting action of the exit side guide to the slab. Figure 18h shows a symmetric compressive rolling stress distribution again similar to that in Figure 18e.

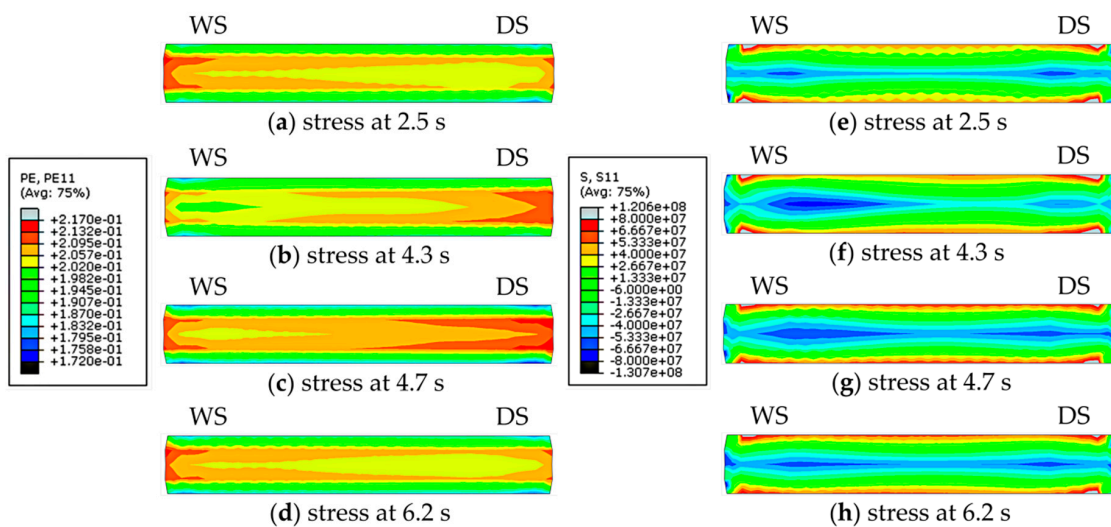


Figure 18. Strain and stress distribution at the exit cross-section of the slab being rolled with exit side guide Separation distance of side guide: 1220 mm.

The effect of the side guide in correcting the camber is also reflected in the roll force distribution over the horizontal roll. As the model of the horizontal roll consists of nine shell rigid elements, the roll force distribution at different moments can be displayed in Figure 19. Since there was an initial slab wedge of 1 mm at the WS, the rolling force at the WS is always greater than that at the DS. At the period between 4.3 s and 4.7 s, during which the side guide was effectively correcting the slab centerline, a slight rise of rolling force at the WS was noted. On the contrary, rolling force decreased slightly at the DS during the period the side guide was actuating between 4.3 s and 4.7 s. An important factor affecting the rolling force distribution across the roller is the leveling of the horizontal rolls, which results in a gap gradient in roll-bite. Leveling is thus a further measure in adjusting the centerline profile; however, it is beyond the scope of this work.

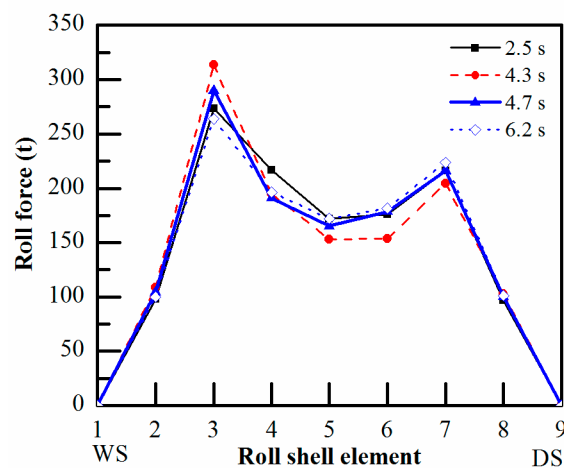


Figure 19. Roll force across the horizontal roller at different moments.

4.4. Additional Discussion

The slab centerline can be effectively corrected as long as the moment acting on the slab head exerted by the exit side guide or the moment acting on the slab end exerted by vertical roll VR3 is maintained. In other words, a longer engaging period of a slab in the exit side guide or a longer engaging period with the vertical roll VR3 could be beneficial in improving the centerline profile. Increasing the length of the exit side guide, for example, would be an effective measure. In addition, by introducing a set of intermediate side guides between the vertical rolls VR3 and horizontal roughing rolls HR2, as implemented in some modern roughing lines, is effective in correcting the centerline profile, especially towards the slab end region. The intermediate side guide prolongs the contact period of the slab end even if the slab end is disengaged from the vertical rolls VR3, therefore, allows a correcting moment exerted on the slab end region. Increasing the engaging period also can be achieved by force-mode side guides [17]. While the slab enters the force-mode side guide, the contact between the side guide and the slab is controlled by maintaining a constant reaction exerted on the slab so that more stable and continuous contact and consequently a more stable force history during the engaging period can be achieved.

5. Conclusions

Finite element simulation was explored to examine the mechanism of the position-mode side guide in correcting the slab centerline profile and camber in the roughing process. This work could be the first to give an insight into the mechanism of side guides in correcting the slab. The following conclusions can be drawn from the results:

- A numerical model of the roughing mill consisting of the roughing stand and side guides was established to visualize the interaction between the moving slab and the associated rough mill components.
- The visualization was realized by time sequence analysis unveiling instantaneous slab positions and the variation of the centerline profile of slab at various moments.
- The characteristics of the reaction history on the slab correlated well with the associated time sequence of the roughing process, which explained the interaction between the roughing mill components and the slab well. The effect of the separation distance of the side guide and the effect of the slab wedge on the centerline profile were predicted. The results were consistent with the on-site data from a CSC roughing line with the same characteristics and in the same order of magnitude.
- A schematic model was proposed to illustrate the reactions and the resulting moments exerted on the slab. Together with the reaction history, the cross-sectional strain/stress distribution and the roll force distribution across the horizontal rolls, the correcting mechanism of the side guide and the vertical rolls on the centerline profile and on the camber of a slab during the roughing process can be elucidated.
- The results of this work also provide a further knowledge base for side guide selection and dimension design to enhance the effectiveness of side guides in correcting the centerline profile and camber.

Author Contributions: Methodology, H.-K.H. and J.-N.A.; software, H.-K.H.; validation, H.-K.H.; formal analysis, H.-K.H.; writing—original draft preparation, H.-K.H. and J.-N.A.; writing—review and editing, H.-K.H. and J.-N.A.; project administration, J.-N.A.

Funding: This research was funded by the Ministry of Science & Technology of R.O.C. (Taiwan) and the China Steel Corporation in Kaohsiung under grant number MOST 102~106-2622-8-006-001 and MOST 107-2218-E-468-004.

Acknowledgments: The Ministry of Science & Technology of R.O.C. (Taiwan) and the China Steel Corporation in Kaohsiung are acknowledged for their support of the funding of this research. The authors are grateful to the Hot Rolling Division of China Steel Corporation (CSC) Kaohsiung for their providing on-site data and for their valuable discussion.

Conflicts of Interest: The authors declare no conflict of interest.

References

1. Shiraishi, T.; Ibata, H.; Mizuta, A.; Nomura, S.; Yoneda, E.; Hirata, K. Relation between camber and wedge in flat rolling under restrictions of lateral movement. *ISIJ Int.* **1991**, *31*, 583–587. [[CrossRef](#)]
2. Montague, R.J.; Watton, J.; Brown, K.J. Centre-line deviation as a measure of camber in steel slabs during unrestricted horizontal rolling. *Proc. Inst. Mech. Eng. Part C J. Mech. Eng. Sci.* **2005**, *219*, 775–783. [[CrossRef](#)]
3. Nilsson, A. FE simulations of camber in hot strip rolling. *J. Mater. Process. Technol.* **1998**, *80*, 325–329. [[CrossRef](#)]
4. Kang, Y.; Choi, Y.J.; Oh, G.; Won, S. Estimation of Camber Generation in Rough Rolling Process. In Proceedings of the IFAC Symposium on Automation in Mining, Mineral and Metal Processing, San Diego, CA, USA, 25–28 August 2013; Volume 46, pp. 436–439.
5. Wang, X.; Li, F.; Li, B.; Dong, L.; Zhang, B. Design and Application of an Optimum Backup Roll Contour Configured with CVC Work Roll in Hot Strip Mill. *ISIJ Int.* **2012**, *52*, 1637–1643. [[CrossRef](#)]
6. Nandan, R.; Rai, R.; Jayakanth, R.; Moitra, S.; Chakraborti, N. Regulating crown and flatness during hot rolling: A multiobjective optimization study using genetic algorithms. *Mater. Manuf. Process.* **2005**, *20*, 459–478. [[CrossRef](#)]
7. Okada, M.; Murayama, K. VSS control of strip steering for hot rolling mills. In Proceedings of the 16th Triennial World Congress, Prague, Czech Republic, 4–8 July 2005; Volume 38, pp. 19–24.
8. Choi, Y.J.; Lee, M.C. PID sliding mode control for steering of lateral moving strip in hot strip rolling. *Int. J. Control Autom. Syst.* **2009**, *7*, 399–407. [[CrossRef](#)]

9. Hol, C.W.J.; Roo, J.; Kampmeijer, L.; Dirkson, T.; Schipper, G.; Maire, M.L.; Lugt, J. Model predictive controller for strip-tracking during tail-out of the finishing mill. *IFAC Proc. Vol.* **2013**, *46*, 397–402.
10. Lee, J.; Choi, Y.J. Development of camber and steering control system in hot strip mill. In Proceedings of the 2014 IEEE Emerging Technology and Factory Automation (ETFA), Barcelona, Spain, 16–19 September 2014.
11. Kwon, W.; Kim, S.; Won, S. Active disturbance rejection control for strip steering control in hot strip finishing mill. *IFAC Pap. Online* **2015**, *48*, 42–47. [[CrossRef](#)]
12. Jepsen, O.N.; Müller, H.A.; Immekus, J. Process and Device for Intentionally Influencing the Geometry of Roughed-Down Strips in a Roughing-Down Stand. U.S. Patent No. US 8,429,943, 30 April 2013.
13. Byon, S.M.; Lee, Y. An investigation on the effect of design parameters of side guide on camber in hot slab rolling. *Mater. Manuf. Process.* **2014**, *29*, 107–114. [[CrossRef](#)]
14. Linghu, K.; Jiang, Z.Y.; Zhao, J.; Li, F.; Wei, D.; Xu, J.; Zhang, X.; Zhao, X. 3D FEM analysis of strip shape during multi-pass rolling in a 6-high CVC cold rolling mill. *Int. J. Adv. Manuf. Technol.* **2014**, *74*, 1733–1745. [[CrossRef](#)]
15. Zhang, F.; Malik, A. A roll-stack contact mechanics model to predict strip profile in rolling mills with asymmetric, continuously variable crown rolls. *J. Manuf. Sci. Eng.* **2018**, *140*, 011008-1–011008-15. [[CrossRef](#)]
16. Del Pozo, D.; López de Lacalle, L.N.; López, J.M.; Hernández, A. Prediction of press/die deformation for an accurate manufacturing of drawing dies. *Int. J. Adv. Manuf. Technol.* **2008**, *37*, 649–656. [[CrossRef](#)]
17. Aoh, J.N.; Hsu, H.K.; Dai, W.T.; Lin, C.Y.; Yeh, Y.L. Numerical simulation on correcting camber and wedge of steel slabs in hot rolling mill. In Proceedings of the 12th Asia-Pacific Conference on Engineering Plasticity and Its Applications, Kaohsiung, Taiwan, 1–5 September 2014.



© 2019 by the authors. Licensee MDPI, Basel, Switzerland. This article is an open access article distributed under the terms and conditions of the Creative Commons Attribution (CC BY) license (<http://creativecommons.org/licenses/by/4.0/>).